Coronal Dimmings and Energetic CMEs in April-May 1998

B.J. Thompson[1], E.W. Cliver[2], N. Nitta[3], C. Delannée[4], J.-P. Delaboudinière[4]

Short title: CORONAL DIMMINGS AND ENERGETIC CMES

Abstract. We have analyzed the coronal dimmings for seven fast (> 600 km/s) coronal mass ejections (CMEs) occurring between 23 April and 9 May which were associated with flares from NOAA active region (AR) 8210. These dimming regions were identified by their strong depletion in coronal emission within a half hour of the estimated time of CME lift-off. They included areas which were as dark as quiescent coronal holes as well as other regions with weaker brightness depletions. We found that the extended dimming areas in these events generally mapped out the apparent "footprint" of the CME. In two of the seven cases, a pair of dimmings were more or less symmetrically positioned north and south of the flare site. In the five remaining cases, the dimmings were most prominent to the north of AR 8210 ($\sim S15$ latitude) and extended well north of the solar equator, consistent with the locations of the CMEs. We discuss the implications of these results for the sigmoid/double dimming/flux rope model of CMEs.

1. Introduction

The series of solar eruptions associated with active region (AR) 8210 during its disk passage in late April / early May in 1998 represent the initial sustained outburst of major activity during solar cycle 23. The seven major CMEs observed between 23 April and 9 May were associated with M- and X-Class soft X-ray flares, an interplanetary shock at Earth, an intense geomagnetic storm, and the onset of the 11-year cosmic ray modulation cycle (Gopalswamy et al., 1999b). In this study, we analyze data from the EUV Imaging Telescope (EIT; Delaboudinière et al., 1995) and the Large Angle Spectroscopic Coronagraph (LASCO; Brueckner et al., 1995) from the Solar and Heliospheric Observatory (SOHO) spacecraft for these seven solar eruptions to investigate the source regions of energetic CMEs.

We focus on the coronal dimming regions which have been identified in EIT data as regions of decreased brightness in the vicinity of the flares associated with CMEs (Thompson et al., 1998, 1999). Such brightness depletions were discovered in Skylab soft X-ray images by Rust (1983, and references therein) who referred to them as "transient coronal holes." Subsequently, Hudson et al. (1996), Sterling and Hudson (1997), and Hudson and Webb (1997) reported such depletions in Yohkoh SXT data and referred to them as coronal "dimmings." A comparison of Yohkoh SXT data and EIT observations for the 7 April 1997 event (Zarro et al., 1999) established that the dimmings resulted from a decrease of coronal density, consistent with Rust's original interpretation (cf., Hudson et al., 1996). The "double dimmings" such as those observed in the well-studied event of 7 April (Sterling and Hudson, 1997; Zarro et al., 1999; Thompson et al., 1999) in which darkened areas appear in the concavities of sigmoid-like structures (Canfield et al., 1999), readily lend themselves to a flux rope interpretation (e.g, Démoulin, Priest and Lonie, 1996; Sterling and Hudson, 1997; Gibson et al., 1999; Titov and Démoulin, 1999). In such a picture, the indents in a sheared (S-shaped) neutral line represent the opposite ends of a flux rope. Upon eruption of the flux rope, the nascent dimming

regions are "opened" to the solar wind and become dark as mass escapes. Thompson et al. (1998) pointed out that "perfect examples" of double dimming regions such as 7 April and 12 May 1997 "are rarely observed in EIT, and often the dimming occurs on only one side of the neutral line, or the entire area near the erupting region shows a decrease in brightness."

Despite the potential significance of the dimming signature as a diagnostic of CME origin, no comprehensive study has yet been undertaken of the relationship of the dimming events to CMEs. Such a project presented itself naturally to the "Arcades and Dimmings" subgroup at the International Solar Terrestrial Physics (ISTP) Workshop On the Global Picture of Eruptive Solar Events. At the Workshop we initiated an investigation of dimmings for each of the 29 interplanetary radio events under Consideration. As a first installment of this study, we decided to address the major CMEs associated with the disk passage of AR 8210. These CMEs, despite originating in the same active region, display great variation which allows us to compare and contrast the eruptions. In all, this active region appears to account for 11 of the 29 workshop events if we include an event from well beyond the west limb on 11 May. We focus on the 10 events occurring between 23 April and 9 May when AR 8210 was either on the disk or near the solar limb. These 10 interplanetary radio events can be traced to seven distinct solar eruptions. Six of these CMEs had speeds > 1000 km/s. Evidence of "EIT Wave" transients (e.g. Thompson et al, 1999) were also observed in each of the seven eruptions.

2. Observations and Analysis

During the disk passage of AR 8210, SOHO EIT images at 195 Å were taken at an average cadence of 17 minutes. Most of the images were full-resolution (2.6 arcsec per pixel), with some periods at half-resolution. The 195 Å bandpass is dominated by an Fe XII emission line, which corresponds to a temperature of 1.5 MK at typical coronal

densities.

The dimming regions for the seven CMEs we considered were defined by examining EIT data over a range of several hours surrounding the eruption. In most cases, the full extent of coronal dimming was not apparent in a single image. Areas exhibited different degrees of decreased emission and different areas could commence dimming at different times. Generally, the maximum spatial extent of the dimming was reached within $\sim$ 30 minutes after the soft X-ray flare peak. What appeared to be EIT wave transients characteristically appeared outside the expansion of the dimming region from the flare site, and the waves typically first appeared in the same image in which the dimming increase was first observed. Unfortunately, the 17-minute cadence made it difficult to determine the exact correspondence between these two phenomena.

Some of these dimmings (particularly the dimming on 6 May) are also strongly evident in the Yohkoh SXT data, implying that the dimmings are at least partially representative of a depletion of coronal material. However, other events show little evidence of dimming in soft X-ray images, indicating that the coronal material can vary in temperature from event to event.

Figure 1 shows the dimming regions for the seven eruptions in the form of "percentage-difference" images. A percentage-difference image represents the percentage change in emission between a reference image and a post-eruption image. Data on the seven events, including the times of the reference images

Some of these dimmings (particularly the dimming on 6 May) are also strongly evident in the Yohkoh SXT data, implying that the dimmings are at least partially representative of a depletion of coronal material. However, other events show little evidence of dimming in soft X-ray images, indicating that the coronal material can vary in temperature from event to event. and the post-eruption images are given in Table 1 (t_{base} and t_{dim}). The advantage of percentage-difference images is that regions of bright emission are not enhanced relative to dimmer regions which are weakly emitting, thus

it is possible to simultaneously note all regions which exhibited a decrease in emission. Each of the images are scaled from a 20 % decrease in emission (black) to a 20 % increase in emission (white). The gray regions represent areas which exhibited little or no fractional change in emission.

Figure 2 shows the non-differenced EIT data for the 2 May 1998 eruption at 12:53 and 14:10 UT, the latter image exhibiting a patchy decrease in emission over a large portion of the visible disk. The EIT 195 Å data best exhibits a decrease in emission in the low ($< 1.2\ R_{\odot}$) corona, in areas that were already strongly emitting in the EUV. Regions that were weakly emitting relative to the background emission level would not be readily identifiable if they experienced a decrease in emission. The weaker background emission in soft X-rays makes dimming regions more difficult to observe at these wavelengths and special processing techniques may be required to reveal the brightness depletion. However, the dimming of transequatorial loops in the 6 May and 9 May eruptions were easily observed in the SXT data. Each of the seven eruptions in our study exhibited strong dimming at 195 Å near the flaring region, but they were also accompanied by other areas which dimmed to a lesser extent.

For two of the seven events, 23 April and 27 April, motions in the corona and/or dimmings were apparent about a half hour before the main phase of the flare began. The early dimming in the 27 April event has been discussed in detail by Gopalswamy et al. (1999a). The 23 April eruption also shows a similar sequence of events, with the dimming to one side of the CME commencing before the flare, while the second dimming progresses with the flare. It should be noted that it is possible to consider these two eruptions as separate events which are occurring close in time; dimmings occur all around AR 8210 during the period of this study, while flares occur at various locations in the region, and it is difficult to determine which are associated and which are coincidental.

We examined the LASCO C2 coronagraph data to identify the white light

counterparts of the EIT dimmings shown in Figure 1. The LASCO C2 coronagraph (2.0 - 6.0 field of view) records the white light brightness of coronal structures and eruptions at an image cadence that typically ranged from 25 to 90 minutes in April and May of 1998. As with the EIT data, the LASCO images were examined in different ways to determine the extents of the CMEs. Running-difference movies were used to highlight the transient features, and standard images were examined to determine the morphology of the eruption without differencing artifacts. For six of the seven events, the angle over which the white light CME ranged (projected radially back to the solar surface) is indicated by the solid arrows in Figure 1. The arrows are omitted for the 2 May, 1998 eruption because the CME brightening extended over a large range. This eruption is a good example of a "halo" CME, typical of eruptions which occur near the solar disk center.

The time of the first appearance of the CME in the LASCO C2 data is given in Table 1 along with the time for which we determined the latitudinal extent of the CME. Because of the ambiguity of the "two-staged" CME's on 27 and 29 April, and because of a previous eruption already in the C2 field of view on 6 May, it is difficult to draw strong conclusions based on the timing of the white light mass ejection and the SXR flare flux. In general, the CME appeared in the LASCO C2 field of view (at $\sim 2\ R_{\odot}$) within a half hour (before or after) of the peak SXR flux.

Similarly, the low cadence of EIT images prevented us from determining the timing of the dimming onset relative to the appearance of the white light CME. However, the EIT dimming commenced within a half hour of the initial appearance of the CME in LASCO C2 in every event.

From the last two columns of the table, it can be seen that our measured angular span is in all cases smaller than that listed on the LASCO list shown in the last column of the table. Four of the seven events are listed as full (360°) haloes on the web page; according to our determination none of the seven CMEs had angular spans >170° (the

2 May 1999 CME angular extent represents the primary loop-shaped feature; including adjacent brightenings result in a measured extent greater than >170°. There are two reasons for this difference. First, we distinguished between new bright regions and deflections or compressions of streamers, which show up as bright regions on differenced images but do not represent the outflow of mass through the corona. Second, we determined the extent of the CME relatively early in the event based on a single image; the full extent of brightening may not be present in every image. Examples illustrating our technique are given in Figure 3(a-d) for four of the events in Table 1. In these composite images, the inner image is the EIT image shown in Figure 1. In Figure 3a, the outer image is the raw (undifferenced) C2 data for the time given in Table 1, while in Figure 3(b-d), the outer image is a subtraction from an earlier image. Of particular interest are the bright and dark streamers in the lower right corner of the outer subtracted image in Figure 3(d). The dark "streamer" results from the displacement of the bright streamer away from the CME in the time between the two images. It is a signature of a deflection/compression event (St. Cyr and Hundhausen, 1988) and helps us to distinguish between the "true" extent of a coronal mass ejection and other dynamically transient features.

A comparison of the outlined dimming regions with the arrows marking the angular extent of the CMEs in Figure 1 (and the EIT dimmings and coronagraph images in Figure 2) suggests that the EIT dimmings mark the source regions of the CMEs. Even for the 27 April event (Gopalswamy et al., 1999a) for which the angle subtended by the dimming regions is much smaller than the angular span of the CME (Figure 1). the composite in Figure 3(b) indicates that the CME observed in LASCO C2 is centered about the EIT dimming and exhibits a reasonable correspondence with the off-limb dimming.

Table 1. Summary of Events Studied

	Flare			Dimming		CME				
Date	t_{GOES}	Flux[a]	Location	t_{base}	t_{dim}	t_0[b]	t_1[c]	v km/s[d]	Θ	Θ_{LASCO}[d]
04/23	05:57	X1.3	S16E90	05:33	06:01	05:27	06:27	1390	103	360
04/27	09:20	X1.1	S16E50	08:06	09:50	08:56	09:56	1631	169	360
04/29	16:37	M7.0	S16E23	15:51	17:03	16:59	17:27	1016	158	360
05/02	13:42	X1.1	S15W15	12:53	14:10	14:06	15:13	1044	106	360
05/03	21:29	M1.5	S15W34	21:09	22:06	22:02	22:27	639	59	240
05/06	08:09	X2.8	S11W65	07:58	08:38	08:05	09:02	1053	93	185
05/09	03:40	M7.8	S11W90	03:11	04:02	03:36	04:10	1726	75	143

[a]Mm.n and Xm.n stand for peak X-ray fluxes of m.n$\times 10^{-5}$ W/m^2 and m.n$\times 10^{-5}$ W/m^2, respectively, as measured in the 1–8 Å channel of the GOES detector.

[b]Time of the LASCO C2 image in which the CME is first recognized.

[c]Time of the LASCO C2 image in which the angular extent of the CME is measured.

[d]From the LASCO CME list compiled by O.C. St. Cyr and S.P. Plunkett (1999).

The angular extent of the arrows in Figure 1 is listed in the θ column of Table 1, along with the time (t_1) that the measurements were made.

3. Discussion and Conclusions

Typical CME angular extents are much larger than the 20-30° longitudinal span of major active regions. The average CME span is ~45° (Hundhausen, 1993); for CMEs associated with kilometric Type II bursts the median span is ~ 90° (Cane et al., 1987).

Until now, no chromospheric or coronal feature of comparable angular size with the CME has been identified as a signature of the source region for energetic (massive, fast) CMEs associated with active region flares. We submit that the EIT dimming regions which appear to crudely map the "footprint" of the major CMEs associated with AR 8210 in April and May 1998 represent such a diagnostic. We note the behavior observed for the last five events in the series from AR 8210 is consistent with those identified by Harrison et al. (1990), who found that CMEs often lay to one side of the flaring active region.

In all 7 events in our study, the dimming regions extend well away from the flare site in AR 8210 and appear to correspond to the white light extent of the CME better than the flare location. For the last five events in the sequence, occurring between 27 April and 9 May, the principal northward expansion of the dimming regions corresponds to the observed location of the CME relative to the active region. The first two events, which exhibited either a launch which preceded the flare as described by Gopalswamy et al. (1999a) or consisted of a multi-part eruption of a closely-spaced sequence of two eruptions, display an angular extent far to the south of the flaring active region. In these two events, the white light extent of the CME also extended far south of the active region. Thus, the first two white light events appear to be centered about the flaring region, while the following five exhibit a flare at one "leg," as observed by Harrison et al. (1990).

Because of the low image cadence in EUV and white light, it is sometimes not possible to declare whether one phenomenon led or preceded another. However, the timing of the different aspects of the eruption were fairly close - the peak soft X-ray flux generally occurred within a half hour of the first observation of the CME in the LASCO C2 data, and the dimming in the EIT images commenced within a half hour of the appearance of the CME in LASCO C2.

Some caveats apply. The workshop events are biased toward the most energetic

eruptions. Assuming at least a rough correlation between the CME mass and the extent of the dimming (e.g., Gopalswamy and Hanaoka, 1998), such eruptions are those most likely to exhibit brightness depletions in EIT. We have conducted a detailed analysis for only 7 of the 29 workshop events with EIT and LASCO coverage. A preliminary examination of the remaining events supports our conclusion and the full results will be reported elsewhere. Additionally, there were a number of eruptions which occurred during this period which were not accompanied by interplanetary type II or IV bursts; these CMEs should be investigated before conclusions can be drawn about whether dimmings and EIT waves are associated with the radio bursts.

What are the implications of the extended dimmings for the sigmoid / double dimming / flux rope model? If the transient coronal holes in the concavities of the sigmoid represents the ends of a flux rope, then to what do the extended dimmings in the last five events in the April/May 1998 sequence correspond? The eruptions earlier in the cycle such as that of 7 April 1997 may provide insight. In that case the magnetic source region on the Sun was less magnetically complex, and there were few strong magnetic regions on the Sun at that time. The associated double dimmings were well-defined and remained relatively close to the active region. Between 23 April and 9 May 1998, however, the magnetic structure of the surface of the Sun was more complex. In particular, after 30 April active region 8214 ($\sim$ N26 latitude), which lagged $\sim$40° behind AR 8210 in longitude evolved rapidly (Figure 1). The coronal depletions for the last five events in Table 1 all extended north and east towards this active region.

A similar north-and-south active region geometry held for a shorter sequence of three major CMEs in early November that has been studied in detail by Delannée et al. (1999). They showed that transequatorial loops (observed in EIT) which linked the principal flaring region and magnetic regions on the opposite side of the equator faded from visibility of disappeared in conjunction with the CMEs and were replaced by dimming regions. Thus the underlying magnetic geometry of CMEs at solar maximum

- when active regions characteristically appear on both sides of the equator - is likely more complicated than those earlier in the cycle, e.g., for April 1997, and can involve connections between widespread magnetic regions.

The nature of the extended dimming regions in these events remains unclear and would benefit from further study. Their general appearance and location, lying between or outside of active regions, complicates the interpretation in terms of a simple sigmoid/flux rope model. In addition, the relationship of the EIT waves to the extended dimmings remains to be determined. For the present, however, based on the general correspondence between the locations of coronal depletions and CMEs observed in the energetic April-May 1998 events (Figures 1 and 3), we regard the extended dimming regions as a signature of CME source regions, i.e., areas where previously closed flux has been opened to the interplanetary medium. Such regions may, of course, include or encompass a flux rope topology.

Acknowledgments. We thank Nat Gopalswamy and Jim Green for organizing a stimulating and productive ISTP/IACG workshop. NN's work was supported by NASA contract NAS 8-40801.

References

Brueckner, G.E. et al., *Solar Phys., 162,* 357-402, 1995.

Cane, H.V., N.R. Sheeley, Jr., and R.A. Howard, *J. Geophys. Res., 92,* 9869-9874, 1987.

Canfield, R. C., H. S. Hudson, and D. E. McKenzie, *Geophys. Res. Lett., 26,* 627, 1999.

Delaboudinière, J.-P. et al., *Solar Phys., 162,* 291, 1995.

Delannée et al., submitted to *Solar Phys.*, 1999.

Démoulin, P., E. R. Priest, and D. P. Lonie, *J. Geophys. Res. 101,* A4, 7631, 1999.

Gibson, S.E., A. Alexander, D. Biesecker, R. Fisher, M. Guhathakurta, H. Hudson, and B.J. Thompson, *Solar Wind Nine,* eds., S. R. Habbal, R. Esser, J.V. Hollweg, and P.A. Isenberg, AIP Conf. Proc. 471 (AIP: Woodbury, NY) pp. 645-648, 1999.

Gopalswamy et al., *Geophys. Res. Lett.*, this issue, 1999b.

Gopalswamy, N., and Y. Hanaoka, *Astrophys. J., 498,* L179-182, 1998.

Gopalswamy, N., M.L. Kaiser, R.J. MacDowall, M.J. Reiner, B.J. Thompson, and O.C. St. Cyr, in *Solar Wind Nine,* eds., S. R. Habbal, R. Esser, J.V. Hollweg, and P.A. Isenberg, AIP Conf. Proc. 471 (AIP: Woodbury, NY) pp. 641-644, 1999a.

Harrison, R. A., E. Hildner, A. J. Hundhausen, D. G. Sime and G. M. Simnett,*Astron. and Astrophys. 95,* 917-937, 1990.

Hudson, H.S., L.W. Acton, and S.L. Freeland, *Astrophys. J., 470,* 629-635, 1996.

Hudson, H.S., and D.F. Webb, *Coronal Mass Ejections,* edited by N.U. Crooker, J. Joselyn and J. Feynman, *American Geophysical Union,* pp. 27-38, 1997.

Hundhausen, A.J., *J. Geophys. Res., 98,* 13177- 13200, 1993.

Rust, D.M., *Space Science Reviews, 34,* 21-36, 1983.

St. Cyr, O.C., and A.J. Hundhausen, *Proc. of Sixth Int. Solar Wind Conf.,* eds., V.J. Pizzo, T.E. Holzer, and D.G. Sime (NCAR: Boulder, CO) NCAR/TN-306+Proc, vol. 1, pp. 235-238, 1987.

St. Cyr, O. C. and S. P. Plunkett, on-line LASCO CME List, 1999.

Sterling, A. C. and Hudson, H. S., *Astrophys. J. (Lett.), 491,* 55-58, 1997.

Thompson, B. J., O. C. St. Cyr, S. P. Plunkett, J. B. Gurman, N. Gopalswamy, H. S.

Hudson, R. A. Howard, D. J. Michels, and J.-P. Delaboudinère, in *Sun-Earth Plasma Connections*, edited by J. L. Burch, R. L. Carovillano, and S. K. Antiochos, Geophysical Monograph 109 (AGU: Washington, DC), pp. 31-46, 1999a.

Thompson, B.J., J. S. Newmark, J. B. Gurman, W. Neupert, J.-P. Delaboudinière, O. C. St. Cyr, S. Stezelberger, K. P. Dere, R. A. Howard, D. J. Michels, *Astrophys. J. (Lett.), 517,* L151-L154, 1999.

Titov, V. S. and P. Démoulin, *Astron. & Astrophys.*, 1999, in press.

Zarro, D.M., A.C. Sterling, B.J. Thompson, H.S. Hudson. and N. Nitta, *Astrophys. J.* (submitted) 1999.

B.J. Thompson, E.W. Cliver, N. Nitta, C. Delannée, and J.-P. Delaboudinière, NASA Goddard Space Flight Center, Code 682.3, Greenbelt, MD 20771. (e-mail: Barbara.Thompson@gsfc.nasa.gov)

AFRL/VSBS, Hanscom AFB, MA 01731-3010. (e-mail: cliver@plh.af.mil)

Lockheed Martin Solar & Astrophysics Laboratory, O/L9-41, B/252, 3251 Hanover Street, Palo Alto, CA 94304. (e-mail: nitta@lmsal.com)

Received _____

[1]NASA Goddard Space Flight Center, Greenbelt, MD

[2]Air Force Research Laboratory, Hanscom AFB, MA

[3]Lockheed Martin Solar and Astrophysics Lab, Palo Alto, CA

[4]Inst. d'Astrophysique Spatiale, Orsay, France

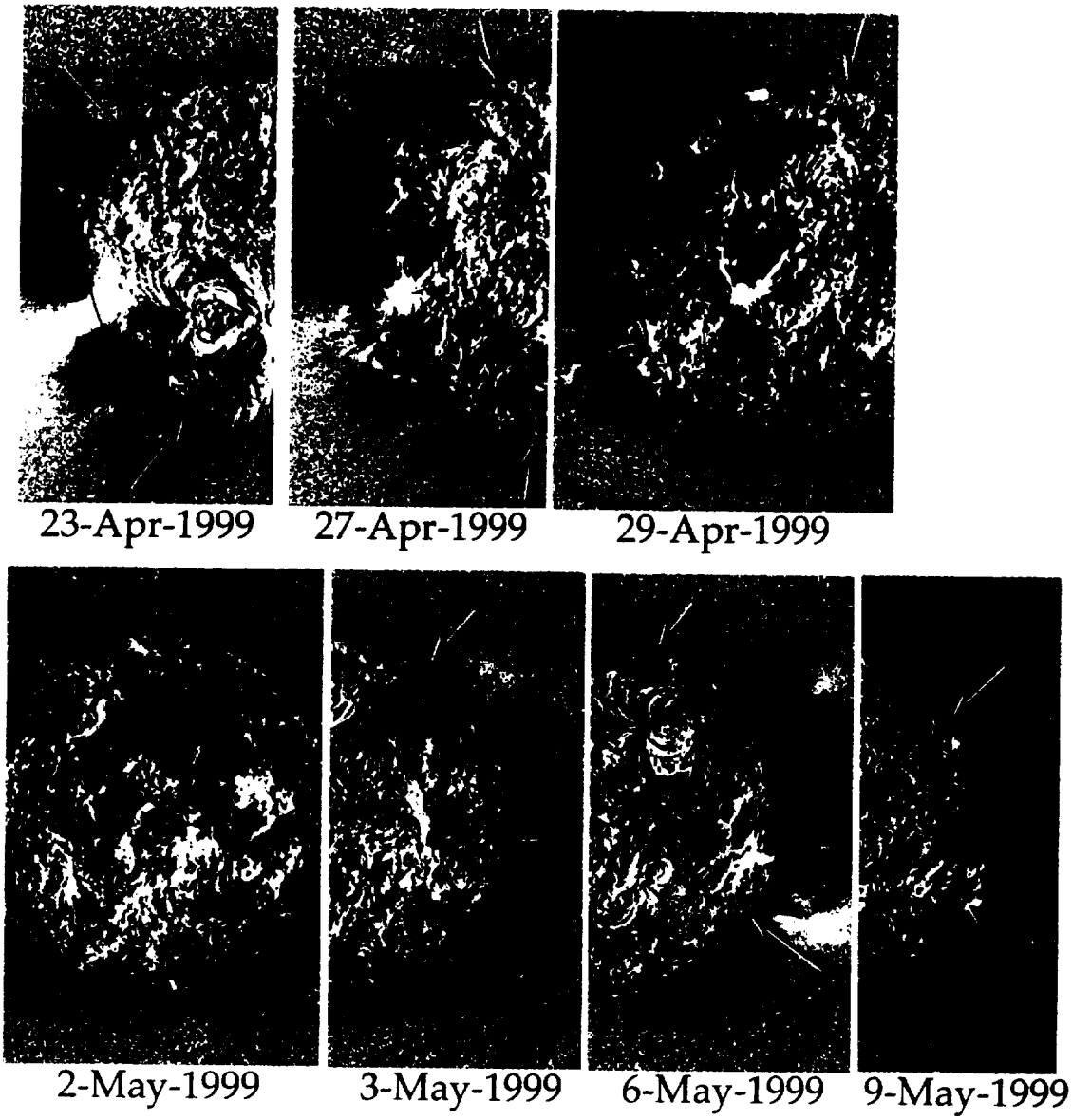

Figure 1. SOHO/EIT "percentage-difference" images in Fe XII 195 Å for each of the events listed in Table 1. A percentage-difference image consists of the fractional change in emission between a pre-event image (recorded at t_{base} in Table 1) and a later image (t_{dim}).
The arrows mark the primary angular extent of the CME identified in the SOHO/LASCO C2 data, projected radially to the solar limb in the EIT images.

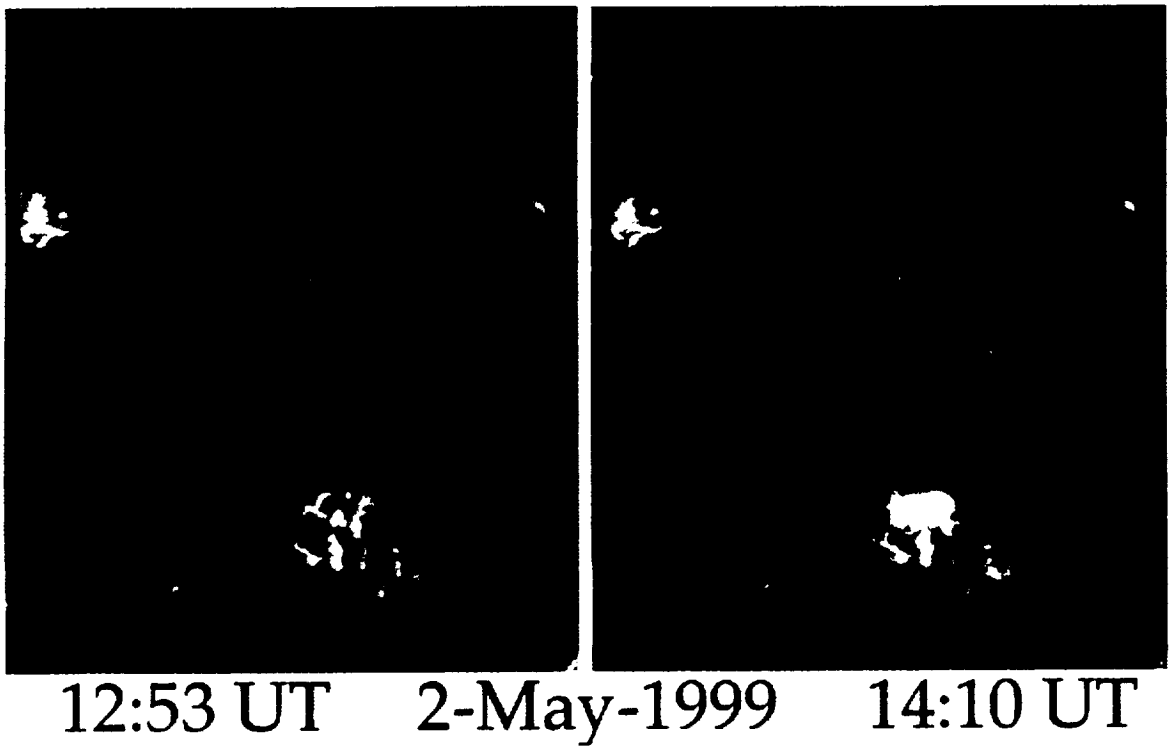

Figure 2. SOHO/EIT Fe XII 195 Å images recorded before and after the eruption on May 2, 1998. The second image (14:10 UT) shows regions of significantly decreased emission compared to the first image (12:53 UT). The fractional change in emission is represented in the fourth frame of Figure 1.

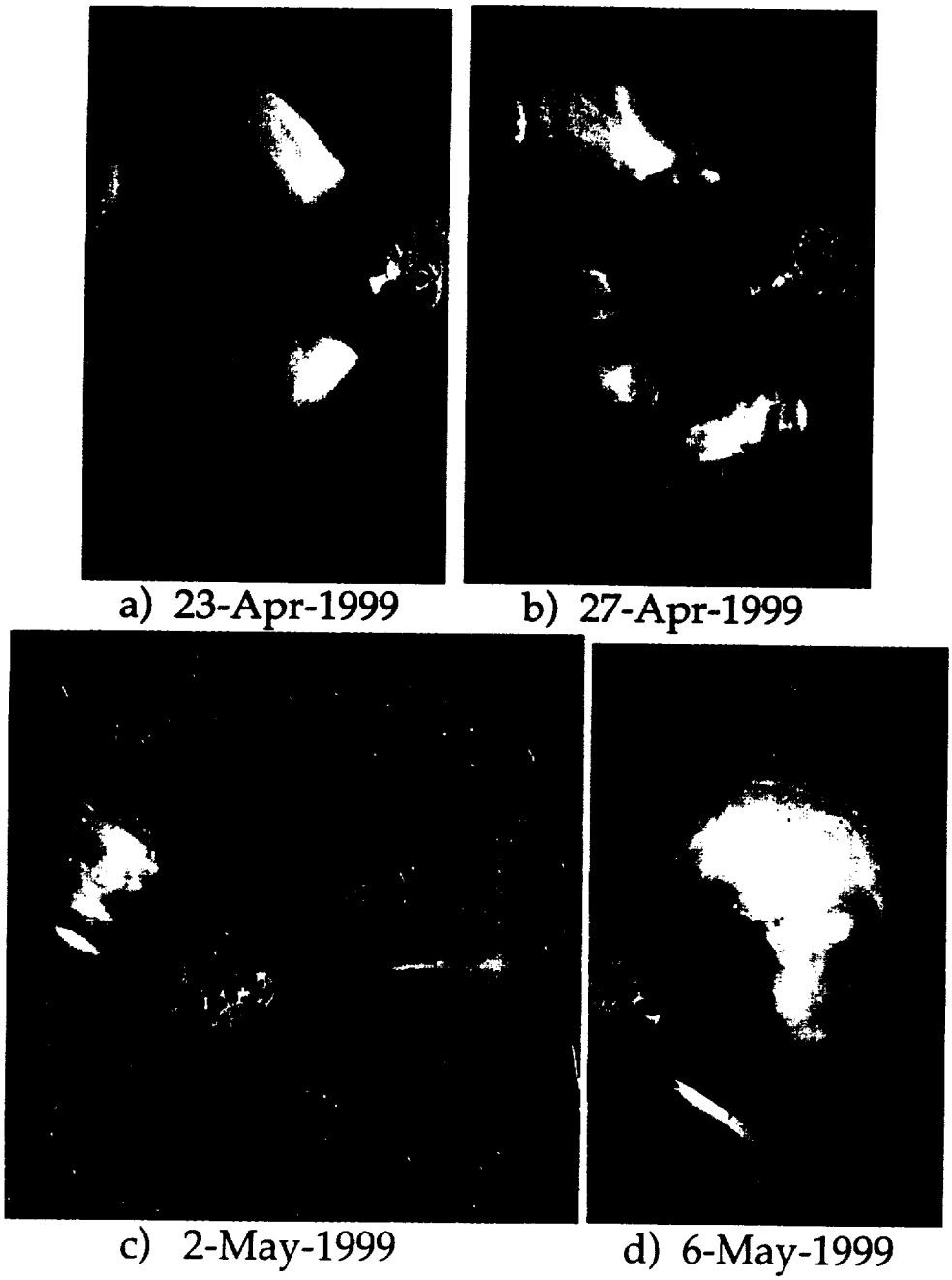

Figure 3. SOHO/EIT percentage-difference images from Figure 1 combined with SOHO/LASCO C2 data for the same eruption. Four CMEs are shown to illustrate a variety of viewing angles and CME structures. The first two images (23 April and 27 April) show strong evidence of dimming both to the north and south of the flaring region; the CME extent in white light displays a similar expanse. The fourth image (6 May) consists of a white light CME and dimming which appear primarily to the north of the flaring region; a bright streamer structure is shown to be deflected to the south of the region. The third figure (2 May) is a "halo" CME, with the flare and dimming occurring closer to disk center.